Asian Journal of Green Chemistry 2 (2018) 189-200

Contents lists available at Avicenna Publishing Corporation (APC)

Asian Journal of Green Chemistry

Journal homepage: www.ajgreenchem.com

Orginal Research Article

Modification of montmorillonite clay with 2-mercaptobenzimidazole and investigation of their antimicrobial properties

Milad Edraki, Davood Zaarei*

Polymer Department, Technical Faculty, South Tehran Branch, Islamic Azad University, P.O. Box 11365-4435, Tehran, Iran

ARTICLE INFORMATION

Received: 13 January 2018
Received in revised: 19 February 2018
Accepted: 19 February 2018
Available online: 27 February 2018

DOI: 10.22034/ajgc.2018.61073

KEYWORDS

Antimicrobial properties
Montmorillonite
Azole
Hybrid nanocompounds
SEM

ABSTRACT

In this study, hybrid synthesized compounds were produced by the interaction between Sodium Montmorillonite clay (Na^+-MMT) inorganic substance and of 2-mercaptobenzimidazole (MBI) organic substance. In this regard, 2-mercaptobenzimidazole was dissolved in ethanol solvent. The addition of clay, timing and also mixing process accelerated the penetration of MBI organic substance into the interlayers spacing of Na^+-MMT and a chemical reaction occurred between the functional groups of these two substances. Small-angle X-ray scattering test (SAXS), fourier transform infrared spectroscopy (FT-IR) and scanning electron microscope (SEM) were used for validation of the interaction between the substances and determining the new structure. The antimicrobial properties of the hybrid synthesized compound against two types of bacteria, two types of fungus and one type of yeast were examined using well diffusion agar method and minimum inhibitory concentration (MIC). The diameter of inhibition zone was measured and their antimicrobial potential was compared with two common antibiotics: gentamicin and rifampin.

Corresponding author, email: d_zarei@azad.ac.ir (D. Zaarei).
Tel.: +9821 33722831.

Graphical Abstract

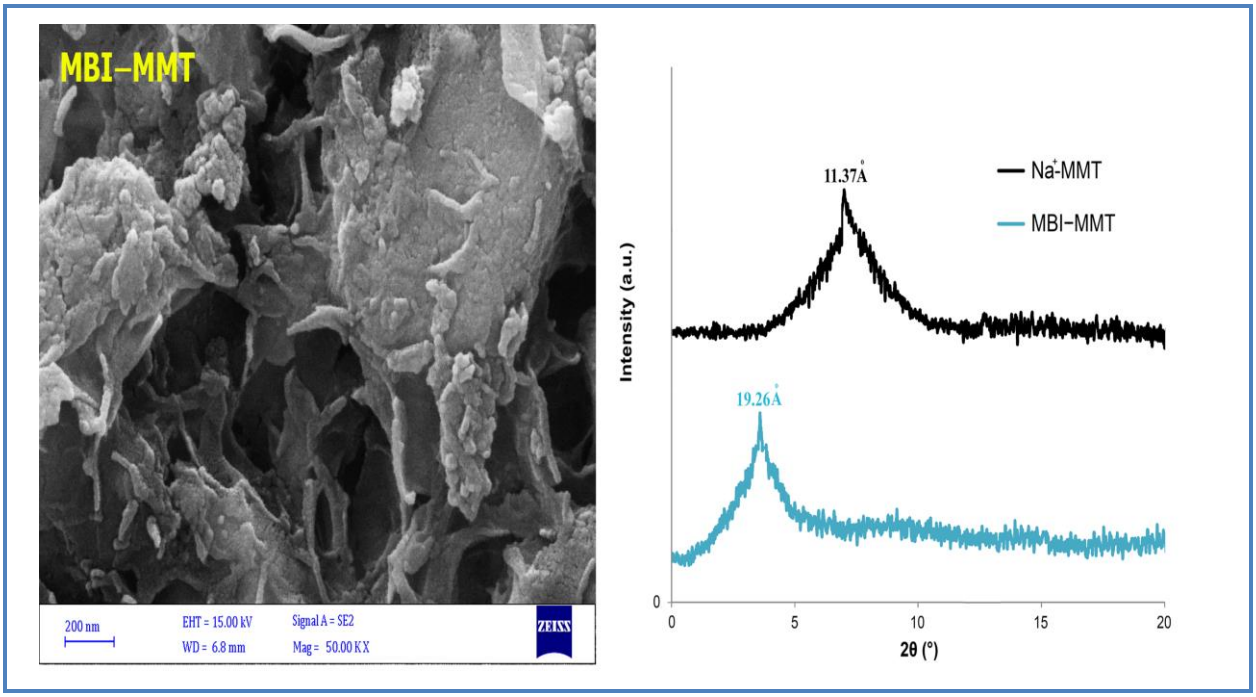

Introduction

During the recent years, bacteria have become highly resistant to antibiotics. On the one hand, the rate of making a stronger antibiotic for replacement is by no means responsive to the increased rate of bacterial resistance. The urgent need for new approaches to deal with bacterial infections is very obvious. One way to fight these microbial agents is to replace the safe antibacterial agents against which the microbial species are not resistant yet [1].

During the past two decades, using azole organic compounds in oil, gas and pharmaceutical industries have attracted a lot of attention since these compounds have many unique properties including excellent corrosion inhibition in various metal surfaces [2–6], antifungal and antibacterial [7–9] properties as well as anti-inflammatory [10] and anti-cancer properties [11].

If these compounds are directly added to paint formulations as a corrosion inhibitor, due to the good solubility of these inhibitors, they can protect the metal surface in a short amount of time; but because of the fast release in corrosive environment the inhibitor concentration in the coating is reduced which results in osmotic pressure and finally blistering and discretization of organic coatings [12, 13]. On the other hand, in polymeric coatings in a temperature condition above 250 °C, due to the heat load on the molecular structure of these organic compounds, their structure becomes destroyed and they lose their function. Also, they should be encapsulated in the pharmaceutical industry for the purpose of their controlled release.

One of the least studied carriers which function based on ion exchange reaction is sodium montmorillonite clay nanoparticles. This inorganic compound is formed of silicate layers with a diameter of approximately 100 nanometers and a thickness of 1 nanometer and include an octagonal plate of ammonium hydroxide or magnesium which is placed in two interwoven tetrahedron silicate layers [14, 15].

In the current study, MBI-MMT hybrid compounds were identified using small-angle x-ray scattering (SAXS), fourier-transform infrared spectroscopy (FT-IR) and scanning electron microscope (SEM). Finally, well diffusion agar and minimum inhibitory concentration methods were used for assessing the anti-bacterial properties of the hybrid nano-compounds.

Experimental

Materials and methods

2-Mercaptobenzimidazole (MBI), deionized water and ethyl alcohol were supplied by Merck Company (Germany). The inorganic clay used in this study was sodium Montmorillonite (Na^+-MMT) and this material was purchased from Rockwood Company (USA). According to the assigned objectives, x-ray diffraction (XRD) studies on the Na^+-MMT and the hybrid synthesized compounds were carried out by employing a Bruker SAXS D8 small angle x-ray diffractometer (Cu-Kα radiation, 40 kV, 35 mA). The data were collected for angles (2θ) from 2° to 20°. The basal spacing d_{001} was calculated from the basal reflections using Bragg's law. FT-IR spectra of Na^+-MMT, MBI and MBI-MMT were run on a VERTEX 70 Bruker company (Germany) by KBr pressed disk method. The spectra were collected for each measurement over the spectral range of 400 to 4000 cm^{-1} with a resolution of 4 cm^{-1}. The morphology of MBI-MMT nano-particles were examined by scanning electron microscope (SEM) made by Germany's ZEISS company (Model sigma VP-500). In SEM test, the mentioned samples were covered with a thin layer of gold and prepared through sputtering method.

Synthesis process

In order to synthesize the compounds, 5 g of Na^+-MMT was dispersed in 350 mL of ethylalcohol and stirred with magnetic stirrer for one hour. This process resulted in the swelling of the clay platelets and the release of exchangeable cations from inter-layer space in solvent environment. In another vessel, 2 g of MBI was dissolved in 100 mL of ethyl alcohol by manual mixing, and the resulting mixture was then transferred to the first vessel. This solution was stirred with magnetic stirrer for 24 h at room temperature in order to insert MBI molecules into the interlayer space of clay particles. After that, the solution was allowed to be in a stasis position for 48 h to precipitate. For separation of synthesized clay modified compounds, a centrifuge device with 6000 r/min, was used

for 15 min in the last phase, sediments were washed with deionized water and remained in a vacuum oven for 24 h so that a dry and light powder can be produced. Schematic structure of synthesized compound are shown in Figure 1.

Antimicrobial test

One type of Gram-positive bacteria including staphylococcus epidermidis (ATCC 12228) and, one type of Gram-negative bacteria including escherichia coli (ATCC 10536), one type of yeast candida albicans (ATCC 10231), and two types of fungus including aspergillus niger (ATCC 16404) and aspergillus brasiliensis (PTCC 5011). The stages for performing the antimicrobial tests are as follows:

First stage: Well diffusion

Fresh culture was prepared from the mentioned bacteria (Gram-positive and negative). A suspension of 0.5 McFarland was prepared from the bacteria and was lawn cultured on Muller-Hinton Agar culture medium. Wells with a diameter of 6 mm were created in the environment and 10 µL of 30 mg/mL was poured into the wells from the compound of interest. The plates were incubated for 24 h at 37 °C. Thereafter, the plates were examined in terms of zone of inhibition diameter and the results were reported.

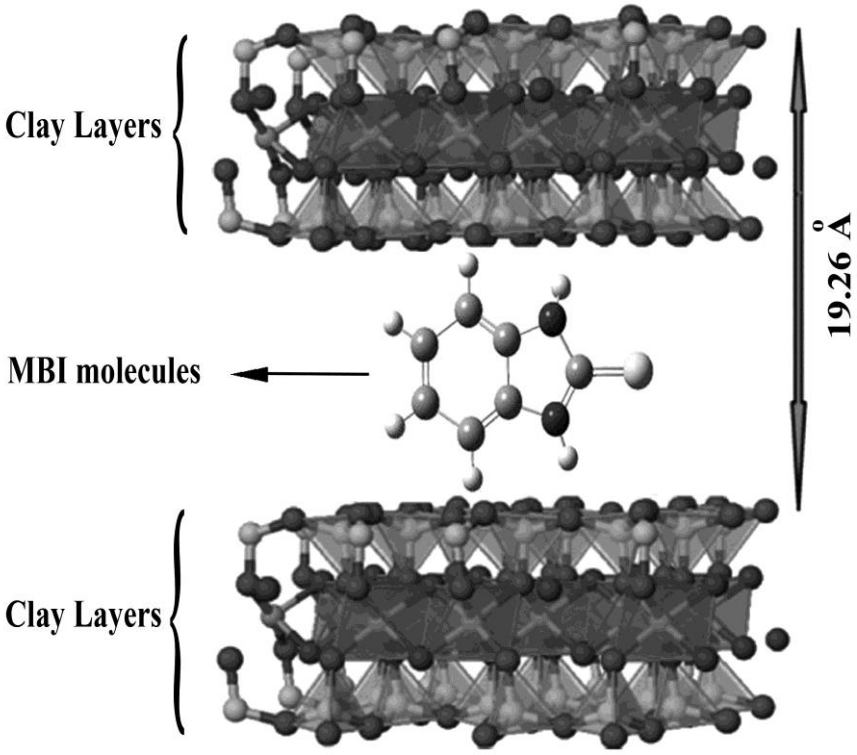

Figure 1. Representation of hybrid synthesized compound

Second stage: Minimum inhibitory concentration (MIC)

Seven dilutions were prepared from MBI-MMT compounds: 2000, 1000, 500, 250, 125, 62.50 and 31.25 μg/mL were the concentrations of the relevant compound. Next, 96-well microplates were used where the microplates had 12 weight-well rows. In each vertical row from top to bottom, seven prepared dilutions as 100 μL were poured. For example, 5 μL bacteria plus 95 μL of the medium tryptic soy broth (TSB) was mixed together with 100 μL from the first dilution.

The third stage: MIC of fungi

The seven dilutions which were used in the previous stage including the minimum inhibitory concentration of the bacteria were mixed with sabouraud dextrose (SD) medium and the prepared plate was inoculated onto the fungi of interest. After the incubation time at 30 °C, the plates were examined in terms of growth of fungi and the last plate in which no fungal growth was observed was also considered as the fungal MIC.

Results and discussion

Small angle x-ray diffraction analysis

Figure 2 illustrates XRD curves for sodium montmorillonite clay (Na^+-MMT) and hybrid synthesized compound (MBI-MMT). As shown in the figure, maximum peak of Na^+-MMT emission is $2\theta=7.4°$ about. Based on the Braggs law, d-spacing is about d=11.37 Å.

X-ray diffraction curve of MBI-MMT depicts that the emission peak is about 4.5°; therefore, the d-spacing (d_{001}) was about 19.26 Å. This reveals that 2 mercaptobenzimidazole (MBI) molecules have penetrated into the interlayer space (galleries) of nanoclay. As a result, d-spacing was increased up to about 7.89 Å. Diffraction characteristics of sodium montmorillonite nanoclay and hybrid synthesized compounds are shown in Table 1.

Fourier transform infrared spectroscopy

Figure 3 clearly shows the FT-IR spectrum for **a**) Na^+-MMT, **b**) MBI, and **c**) MBI-MMT. As shown in the Figure 3**a**, for Na^+-MMT , 465.8 cm^{-1} peak demonstrates Si–O bending vibration (In plane) group; 525 cm^{-1}peak illustrates Si–O–Al vibration and MgO group; 621.9 cm^{-1}peak indicates Mg–O–Si or Fe–O–Si groups; 799.5 cm^{-1} peak shows AlMgOH vibration group; 917.4 cm^{-1} peak shows Al_2OH bending group; 1044 cm^{-1} peak reveals Si–O stretching vibration (In plane) group; 1638.2, 1702.3 and 3448 cm^{-1} peaks depict O–H bending and stretching vibration groups, and finally, 3632.6 cm^{-1} peak represents O–H stretching group [16, 17].

In MBI, an organic corrosion inhibitor, 419.1, 478.2, 597.1, and 654.5 cm^{-1} peaks indicate C–S group; 706, 740.4, 919.3, 1012.3, and 1175.6 cm^{-1} peaks show N–C=S group; 1216, 1261.09, 1354.3, and 1462.6 cm^{-1} peaks reveal C–N–H group; 1511.4 and 1562.9 cm^{-1} peaksrepresents aromatic C=C group; 1622.2, 1696.5, 1743.4, 1834.1, 1871.1, and 1918 cm^{-1} peaks depict C=N group; 2364.4, 2447.8, 2567.9 and 2763.4 cm^{-1} peaks display S–H group; 2876.2 and 2979.1 peaks demonstrate aromatic C–H group and finally, 3112.8, 3155.7, 3617.2, 3677.3, 3743.5, and 3858 cm^{-1} peaks show N–H groups [18, 19].

However, in synthesized MBI-MMT substance, 468.3 cm^{-1} peak reveal Si–O bending vibration group (In plane); 525.6 cm^{-1} peak indicates Si–O–AL vibration and MgO group; 598.3 and 654.3 cm^{-1} peaks depict C–S group; 707.8, 740.7, 918.4, and 1175.9 cm^{-1} peaks show N–C=S group; 799 cm^{-1} peak display Al–Mg–OH vibration group; 1042.7 cm^{-1} peakillustrates Si–O stretching vibration group (In plane); 1260.8, 1355 and 1463.3 cm^{-1} peaks show C–N–H group; 1511.9 cm^{-1} peak demonstrates aromatic C=C group; 1629.6, 1870.8 and 1918.4 cm^{-1} peaks display C=N group; 2448.6, 2568.8, and 2764.1 cm^{-1} peaks reveal S–H group; 2870.2, and 2980.8 cm^{-1} peaks represent aromatic C–H group; 3114.8, 3156.6, 3741.9, and 3844.3 cm^{-1} peaks show N–H group and finally, 3448 and 3623.8 cm^{-1} peaks indicate O–H bending and stretching vibration group. The type of this interaction is hydrogen bond, since S–H group of hydrogen in MBI forms a hydrogen bond with the O–H group inside the structure of Na^+-MMT and the relevant peak can be observed in the frequency of 3448, and 3633 cm^{-1}.

Scanning electron microscope of synthesized compounds

Figure 4 depicts the SEM images of Na^+-MMT, MBI and MBI-MMT with different magnifications. Figure 4**a** and 4**b** indicate the dense sheet-like structure of Na^+-MMT particles. Moreover, Figures 4**c** and 4**d** show the intertwined thread-like structure of MBI organic compounds. In Figures 4**e** and 4**f**, the hybrid structure (Thread-like and sheet-like) with nanometer dimensions can be seen, indicating the interaction between MBI and Na^+-MMT compounds. These pictures are in compliance with XRD and FT-IR tests.

Evaluation of the antimicrobial properties of MBI-MMT hybrid nanocompound

In Table 2, given the sterilized conditions, the performance of the five types of microorganism in the presence of two common antibiotics: gentamicin and rifampin as control, are provided [20, 21]. As shown in Table 2, at MIC point, the performance of these two bacterial inhibitory compounds ranged between 250 and 500 μg/mL whose changes give the type of bacteria. It is noteworthy that

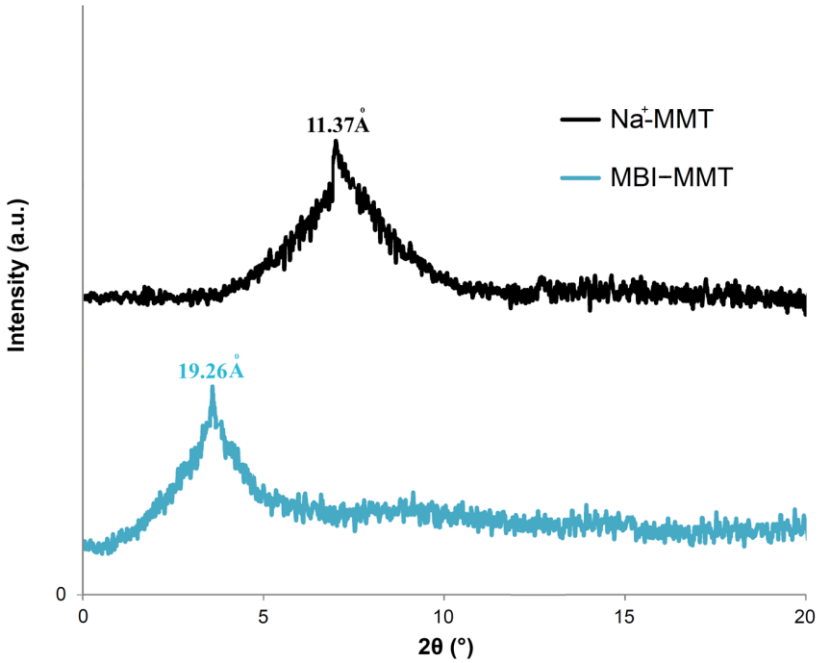

Figure 2. XRD patterns of Na^+-MMT clay and MBI-MMT

Table 1. Interlayer distances of Na^+ - MMT and MBI-MMT system obtained by XRD

Samples	2θ°	d_{001}[Å]	Δd [Å]
Na^+ - MMT	7.4	11.37	7.89
MBI- MMT	4.5	19.26	

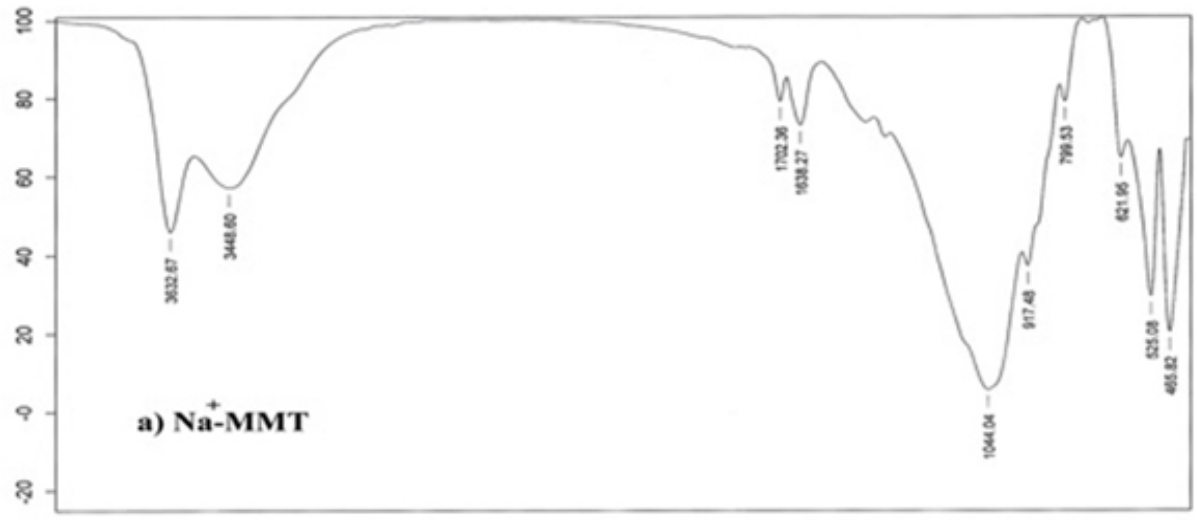

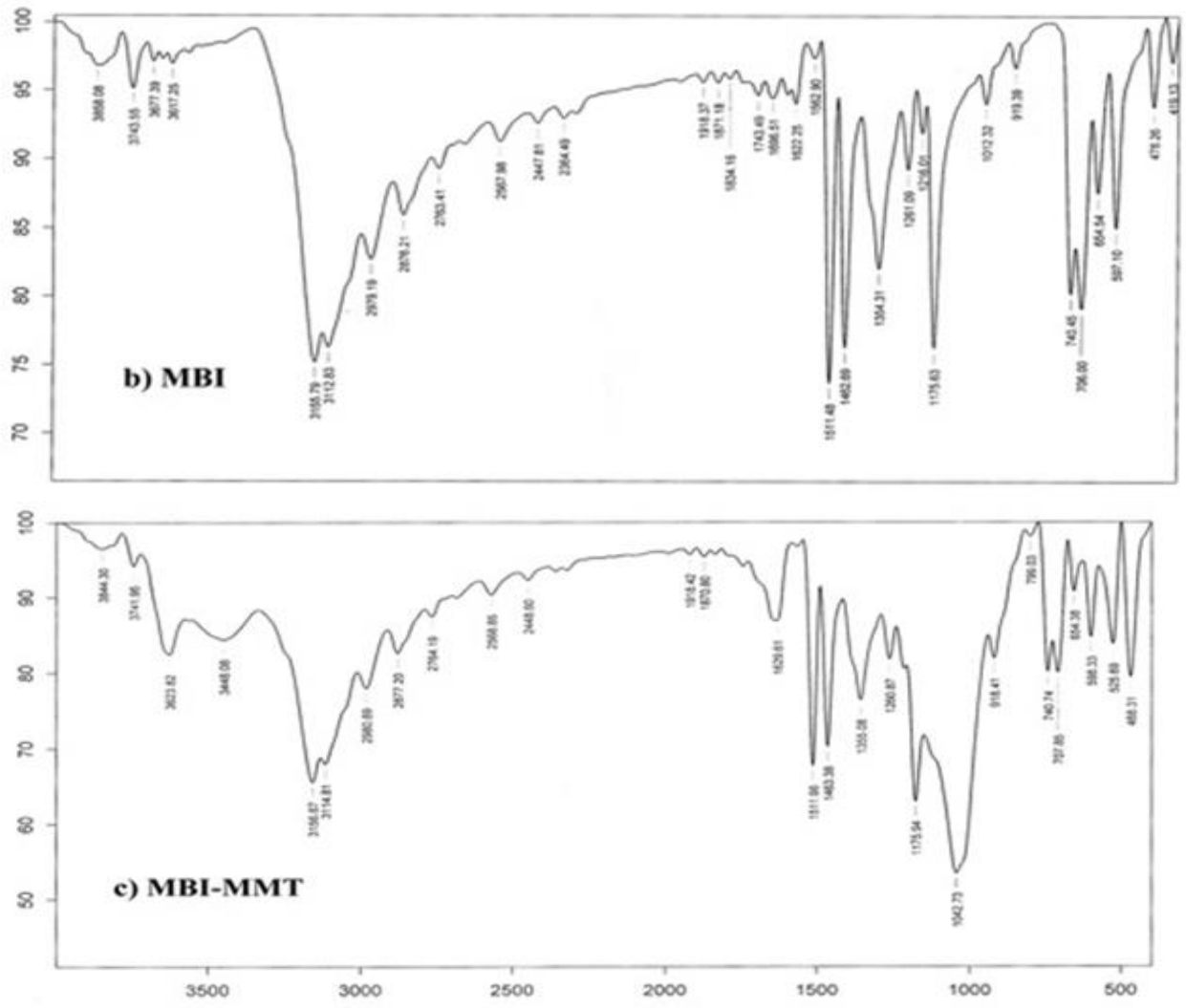

Figure 3. FTIR spectra of a) Na^+-MMT, b) MBI, and c) MBI-MMT

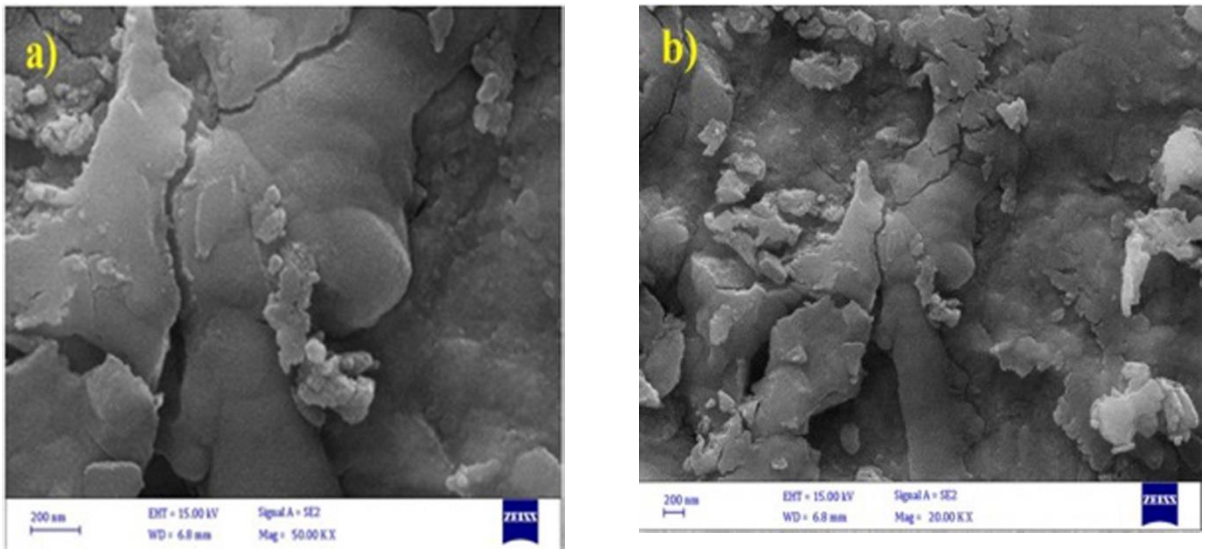

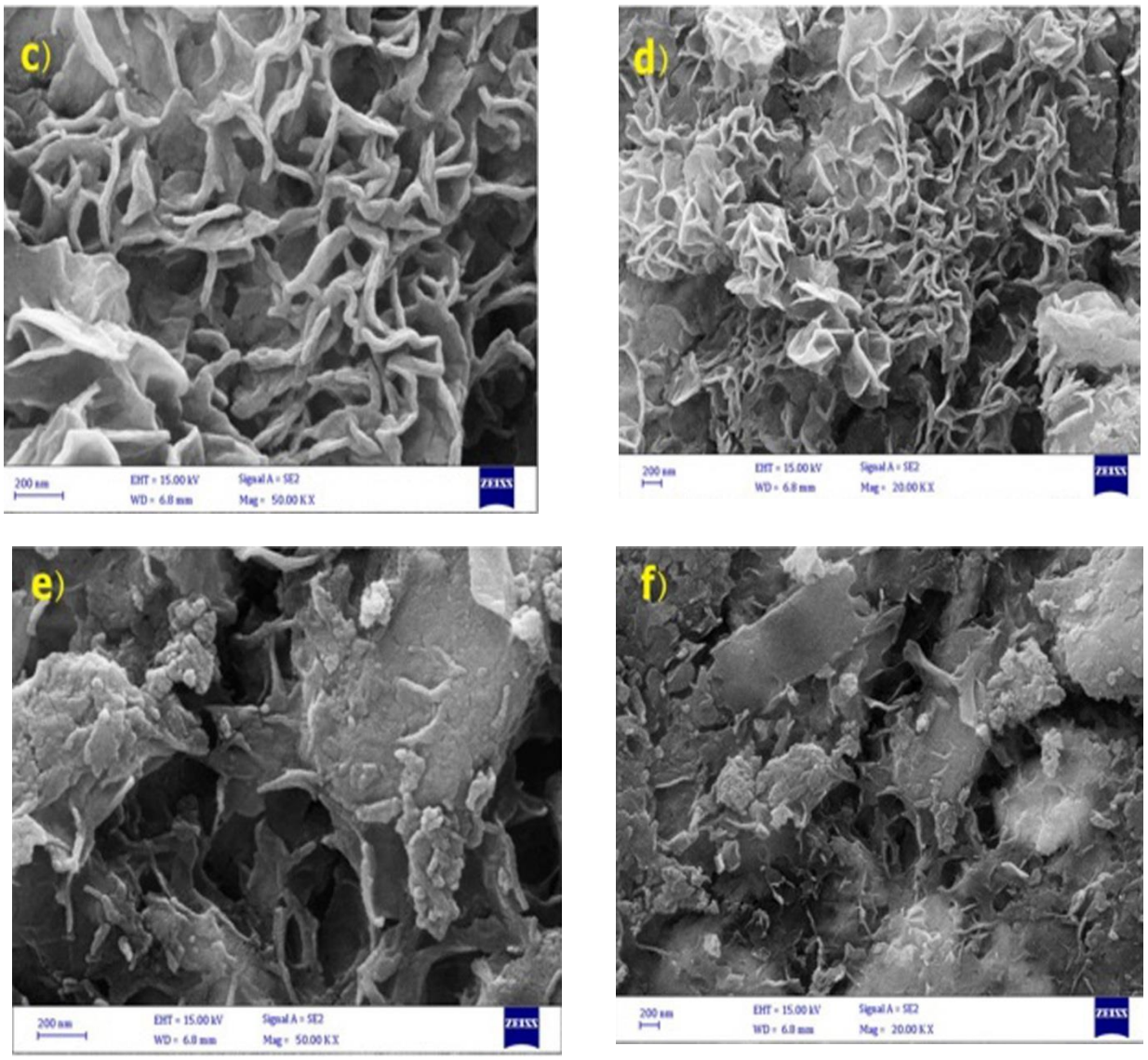

Figure 4. SEM analysis of a) Na^+-MMT sample with magnification of 50X, b) 20X, c) MBI sample with magnification of 50X, d) 20X, e) MBI-MMT sample with magnification of 50X, and f) 20X

in spite of function within the bacterial inhibitory range these two compounds have no function against fungi and yeasts and developed no inhibition [20, 21].

Table 3 provides the minimum inhibitory and bactericidal concentrations for MBI-MMT across the seven prepared concentrations. The results suggest that unlike gentamicin and rifampin, which had no fungicidal function, this compound had this property at very low concentrations of about 62.5 μg/mL. The notable point is that the inhibitory and fungicidal points are at the same concentration, and after this concentration and with its elevation the fungicidal function is completed. In this regard, the minimum inhibitory concentration on the yeast ATCC10231 is about 500 μg/mL which

corresponds to the point of the minimum bactericidal concentration (MBC). The results show that for important bacteria, 1000 μg/mL are required to inhibit the growth and function, where in industrial uses application of this compound (MBI-MMT) should be considered in the coatings.

Table 2. Performance of the common antibiotics in terms of minimum inhibitory concentration under laboratory conditions, on the bacteria, fungi and yeast samples

Antibiotic	Concentration (μg/ mL)	(ATCC 12228)	(ATCC 10536)	(ATCC 10231)	(ATCC 16404)	(PTCC 5011)
Rifampin	250	MIC[a]	growth	NA[b]	NA	NA
	500	B.S[c]	MIC	NA	NA	NA
Gentamicin	250	growth	growth	NA	NA	NA
	500	MIC	MIC	NA	NA	NA

[a] minimum inhibitory concentration

[b] No Active

[c] Bacterio Static

Table 3. The performance of MBI-MMT in terms of minimum inhibitory and bactericidal concentrations, on different microorganisms

Antibiotic	Concentration (μg/ mL)	(ATCC 12228)	(ATCC 10536)	(ATCC 10231)	(ATCC 16404)	(PTCC 5011)
MBI-MMT	31.25	growth	Ineffective	Growth	Growth	Growth
	62.50	growth	Ineffective	Growth	MIC=MBC[a]	MIC=MBC
	125	growth	Ineffective	Growth	-	-
	250	growth	Ineffective	Growth	-	-
	500	growth	Ineffective	MIC=MBC	-	-
	1000	MIC	Ineffective	-	-	-
	2000	MBC	Ineffective	-	-	-

[a] minimum bactericidal concentration

As shown in Table 4, the factor: diameter of inhibition zone suggests the potential of the compound in controlling antibacterial properties. In this regard, the two control compounds: rifampin and gentamicin were examined alongside MBI-MMT. The diameter of inhibition zone for all the samples at MBC or MIC concentrations is provided in the table. As shown, the performance of MBI-MMT is relatively weaker than that of gentamicin, yet it showed better performance and efficiency than rifampin. As rifampin is used as an antibacterial compound in pharmaceuticals, it can

be said that the concentration of about 1000 μg/mL of MBI-MMT has a performance equal to 250 μg/mL of rifampin.

Table 4. The diameter of zone of inhibition in terms of mm at MBC or MIC for MBI-MMT, gentamicin and rifampin, in the presence of different microorganisms

Micro organism	Inhibition zone diameter (mm)		
	(MBI-MMT)	(Gentamicin)	(Rifampin)
ATCC 12228	11	35	40
ATCC 10536	-	21	11
ATCC 10231	17	NA	NA
ATCC 16404	29	NA	NA
PTCC 5011	23	NA	NA

Conclusion

Results of SAXS showed that due to the penetration of MBI organic materials molecules in to the interlayer space of Na^+-MMT, the d-spacing between the clay platlets was increased and intercalation was occurred. Results of FT-IR depicted that after the interaction of MBI with Na^+-MMT, functional groups of MBI organic materials such as, C-S, N-C=S,C-H, S-H , C=C, C-N-H,C=N and tensional N-H have appeared on Na^+-MMT and confirmed the interaction between mineral clay and organic inhibitor. SEM graphs demonstrated the differences in morphology of the modified clays due to the presence of MBI molecules in the synthesized compounds, when compared with neat Na^+-MMT particles. The results of antimicrobial testing for MBI-MMT sample revealed that these compounds had very excellent fungicidal and anti-yeast properties in low concentrations compared to control samples (Rifampin and Gentamicin). Meanwhile, no effect on Gram-negative bacteria (Escherichia coli) was observed, although these compounds were able to successfully inhibit and killed the Gram-positive bacteria (Staphylococcus epidermidis) in higher concentrations.

Disclosure statement

No potential conflict of interest was reported by the authors.

References

[1]. Ren G., Hu D., Cheng E.W., Vargas-Reus M.A., Reip P. Allaker R.P. *Int J Antimicrob Agents.,* 2009, **33**:587

[2]. Markhali B.P., Naderi R., Mahdavian M., Sayebani M. Arman S.Y. *Corros. Sci.,* 2013, **75**:269

[3]. He X., Jiang Y., Li C., Wang W., Hou B., Wu L. *Corros. Sci.,* 2014, **83**:124

[4]. Tang Y., Zhang F., Hu S., Cao Z., Wu Z., Jing W. *Corros. Sci.,* 2013, **74**:271

[5]. Ramezanzadeh B., Ghasemi E., Askari F., Mahdavian M. *Dyes pigm.,* 2015, **122**:331

[6]. Askari F., Ghasemi E., Ramezanzadeh B., Mahdavian M. *Dyespigm.,* 2016, **124**:18

[7]. Azam M.A., Suresh B. *Sci. Pharm.,* 2012, **80**:789

[8]. Mahdi M.F., Al-Smaism R.F., Ibrahim N.W. *Eur. J. Chem.,* 2016, **7:**8

[9]. Kuznetsova A., Domingues P.M., Silva T., Almeida A., Zheludkevich M.L., Tedim J., Ferreira M.G.S., Cunha A. *J. Appl. Microbiol.,* 2017, **122**:1207

[10]. Srivastava S.K., Yadav R., Srivastava S.D. *Indian J. Chem. B.*, 2004, **43**:399

[11]. Bari S., Manda S., Ugale V., Jupally V.R., Akena V. *Indian J. Chem. B.,* 2015, **54**:418

[12]. Ghazi A., Ghasemi E., Mahdavian M., Ramezanzadeh B., Rostami M. *Corros. Sci.,* 2015, **94**:207

[13]. Mehrabian N., Sarabi Dariani A.A. *Polym.Compos.,* 2017, DOI: 10.1002/pc.24492

[14]. Azeez A.A., Rhee K.Y., Park S.J., Hui D. *Composites Part B.,* 2013, **45**:308

[15]. Edraki M., Banimahd Keivani M. *J. Phys. Theor. Chem. IAU Iran.,* 2013, **10**:69

[16]. Kaya M., Onganer Y., Tabak A. *J. Phys. Chem. Solids.,* 2015, **78**:95

[17]. Baron F., SC Pushparaj S., Fontaine C., Sivaiah M., Decarreau A. and Petit S. *Current Microwave Chemistry.,* 2016, **3**:85

[18]. Ahamed M.R., Narren S.F., Sadiq A.S. *Journal of Al-Nahrain University*., 2013, **16**:77

[19]. Al Hokbany N., AlJammaz I., *Open J Inorg Chem.,* 2011, **1**:23

[20]. Ruppen C., Decosterd L., Sendi P. *J. Infect. Dis.,* 2017, **49**:185

[21]. Woźniak-Budych M.J., Przysiecka Ł., Langer K., Peplińska B., Jarek M., Wiesner M., Nowaczyk G., Jurga S. *J. Mater. Sci. Mater. Med.,* 2017, **28**:42

How to cite this manuscript: Milad Edraki, Davood Zaarei*. Modification of montmorillonite clay with 2-mercaptobenzimidazole and investigation of their antimicrobial properties. *Asian Journal of Green Chemistry*, 2018, 2, 189-200. DOI: 10.22034/ajgc.2018.61073